Kinetic Model of Protein-Mediated Ligand Transport: Influence of Soluble Binding Proteins on the Intermembrane Diffusion of a Fluorescent Fatty Acid†

Stephen D. Zucker*

Division of Digestive Diseases, University of Cincinnati, Cincinnati, Ohio 45267

Received June 5, 2000; Revised Manuscript Received October 17, 2000

ABSTRACT: The mechanism (or mechanisms) whereby fatty acids and other amphipathic compounds are transported from the plasma membrane to intracellular sites of biotransformation remains poorly defined. In an attempt to better characterize the role of cytosolic binding proteins in this process, a kinetic model of intermembrane ligand transport was developed in which diffusional transfer of ligand between membrane and protein is assumed. The model was tested by utilizing stopped-flow techniques to monitor the transfer of the fluorescent fatty acid analogue, 12-anthroyloxy stearate (12-AS), between model membrane vesicles. Studies were conducted in the presence or absence of bovine serum albumin (BSA), liver fatty acid-binding protein (L-FABP), and intestinal fatty acid-binding protein (I-FABP) in order to determine the effect of soluble proteins on the rate of intermembrane ligand transfer. As predicted by the model, the initial velocity of 12-AS arrival at the acceptor membrane increases in an asymptotic manner with the acceptor concentration. Furthermore, probe transfer velocity was found to decline asymptotically with increasing concentrations of BSA or L-FABP, proteins that exhibit diffusional transfer kinetics. This observation was found to hold true independent of whether donor or acceptor vesicles were preequilibrated with the protein. In contrast, 12-AS transfer velocity exhibited a linear correlation with the concentration of I-FABP, a protein that is thought to transport fatty acids, at least in part, via a collisional mechanism. Taken together, these findings validate the derived kinetic model of protein-mediated ligand transport and further suggest that the mechanism of ligand−protein interaction is a key determinant of the effect of cytosolic proteins on intracellular ligand diffusion.

The liver cell plays an essential role in the clearance and subsequent metabolism of hydrophobic compounds to more polar metabolites. While the mechanisms underlying the hepatocellular uptake of a host of molecular species has been the subject of intensive investigation (*1*), the processes by which amphipathic ligands are transported through the cytoplasm to intracellular sites of biotransformation remain poorly understood. A variety of soluble, low-molecular-weight proteins capable of binding fatty acids (*2*, *3*), cholesterol (*4*), phospholipids (*5*), and bilirubin (*6*) have been isolated from liver tissue, and it has been proposed that these proteins facilitate the directed transport of their specific ligands through the cell cytosol (*7*, *8*). However, data regarding the influence of cytosolic proteins on the intracellular transport of hydrophobic compounds are conflicting.

The technique of fluorescence recovery after photobleaching (FRAP)[1] has been used to examine the effect of bovine serum albumin (BSA) and liver fatty acid-binding protein (L-FABP) on the diffusion rate of a model fluorescent ligand, NBD-stearate, in model cytoplasm (*9*, *10*) and in cultured cells (*9*, *11*, *12*). A strong correlation between protein binding affinity and diffusion rate was identified, consistent with the proposition that binding proteins enhance diffusive transport by reducing ligand binding to immobile intracellular membranes (*8*). Further support for this hypothesis is derived from the observation that compounds which compete for FABP binding impair the cytoplasmic diffusion of NBD-stearate (*13*) and from the enhanced rates of NBD-stearate diffusion in L cell fibroblasts (*14*, *15*) and mouse embryonic stem cells (*12*) transfected with L-FABP, intestinal FABP (I-FABP), or sterol carrier protein 2. On the other hand, Darimont et al. (*16*) found that overexpression of I-FABP in stably transfected Caco-2 cells inhibited cellular incorporation of radiolabeled palmitate.

Other investigators have attempted to characterize the role of soluble proteins in intracellular transport by studying their effect on the rate of diffusion of amphipathic ligands between model and/or isolated native membrane vesicles. By use of this approach, phosphatidylcholine transfer protein has been shown to stimulate the exchange of *sn*-2 parinaroyl phosphatidylcholine between donor and acceptor membranes (*17*, *18*). Sterol carrier protein 2 also was found to significantly enhance the rate of intermembrane transfer of the fluorescent cholesterol analogue dehydroergosterol (DHE) (*19*, *20*). In contrast, these same investigators demonstrated only minimal

† This study was supported by a National Institutes of Health research grant (DK-51679).

* Address correspondence to this author at the Division of Digestive Diseases, University of Cincinnati, 231 Albert B. Sabin Way, M. L. 0595, Cincinnati, OH 45267-0595. Tel (513) 558-5244; fax (513) 558-1744; e-mail zuckersd@email.uc.edu.

[1] Abbreviations: BSA, bovine serum albumin; DHE, dehydroergosterol; FABP, fatty acid-binding proteins; FRAP, fluorescence recovery after photobleaching; I-FABP, intestinal fatty acid-binding protein; L-FABP, liver fatty acid-binding protein; NBD-PE, *N*-(7-nitro-2,1,3-benzoxadiazol-4-yl)phosphatidylethanolamine; 12-AS, 12-(9-anthroyloxy)stearic acid.

10.1021/bi001277e CCC: $20.00
Published on Web 01/05/2001

enhancement of DHE diffusion in the presence of L-FABP (*19*, *20*). On the basis of the finding that liver cell cytosol stimulates the intermembrane transfer of cholesterol but not β-carotene, Gugger and Erdman (*21*) concluded that carotenoid diffusion is not facilitated by cytosolic proteins. Our own work indicates that increasing the concentration of glutathione S-transferase B (the presumed intracellular carrier protein for bilirubin) causes an asymptotic decline in the rate of transfer of unconjugated bilirubin between model and native hepatocyte membrane vesicles (*22*).

It has been suggested that the conflicting data regarding the effect of cytosolic proteins on the diffusion of amphipathic compounds are a manifestation of differences in diffusion distances between the various experimental systems. This theory holds that vesicle studies generally are performed under conditions where distances over which ligand diffusion occurs are relatively minute and that the effect of binding proteins on ligand diffusion rates is more pronounced when examined over the larger distances present within the cell (*10*). To examine this hypothesis and to better characterize the role of cytosolic proteins in intracellular transport, we developed a kinetic model of protein-mediated intermembrane ligand diffusion in which diffusion distance and ligand and protein diffusion coefficients are considered. We subsequently tested the predictions of the model by analyzing the transfer of the fluorescent fatty acid analogue 12-anthroyloxy stearate (12-AS) between donor and acceptor membranes. The results of these studies suggest that the mechanism of ligand−protein interaction is an essential determinant of the effect of soluble binding proteins on the rate of ligand diffusion.

EXPERIMENTAL PROCEDURES (MATERIALS AND METHODS)

Materials. Grade 1 egg lecithin (phosphatidylcholine) used in the preparation of phospholipid vesicles was obtained from Lipid Products (Surrey, England). The fluorescent stearic acid probe 12-(9-anthroyloxy)stearic acid (12-AS) was purchased from Molecular Probes (Eugene, OR). *N*-(7-Nitro-2,1,3-benzoxadiazol-4-yl)phosphatidylethanolamine (NBD-PE) was obtained from Avanti Polar Lipids (Birmingham, AL). Essentially fatty acid-free bovine serum albumin was purchased from Sigma Chemical Co. (St. Louis, MO). Purified liver and intestinal fatty acid-binding proteins were kindly donated by Dr. Judith Storch. All glassware was washed in chloroform prior to use to eliminate potential lipid contamination.

Preparation of Phospholipid Vesicles. Small unilamellar vesicles were prepared by sonication according to the method of DiCorleto and Zilversmit (*23*), as previously described. A chloroform solution of egg phosphatidylcholine was evaporated to dryness under argon atmosphere, solubilized in diethyl ether, and re-evaporated to form a uniform film. The lipids were desiccated overnight under vacuum to remove traces of solvent and then suspended in a standard buffer containing 0.1 M NaCl and 40 mM Tris (pH 8.1). The lipid suspension was sonicated under argon atmosphere in a bath sonicator (Laboratory Supplies Company, Hicksville, NY) until clear. The mean diameter of vesicles prepared in this manner was 29 nm, as determined by quasielastic light scattering (*24*). NBD-PE was incorporated into acceptor vesicles by cosonication in the presence of phosphatidylcholine at a molar ratio of 10 mol %. Phospholipid concentration was quantified by the lipid phosphorus assay method of Bartlett (*25*).

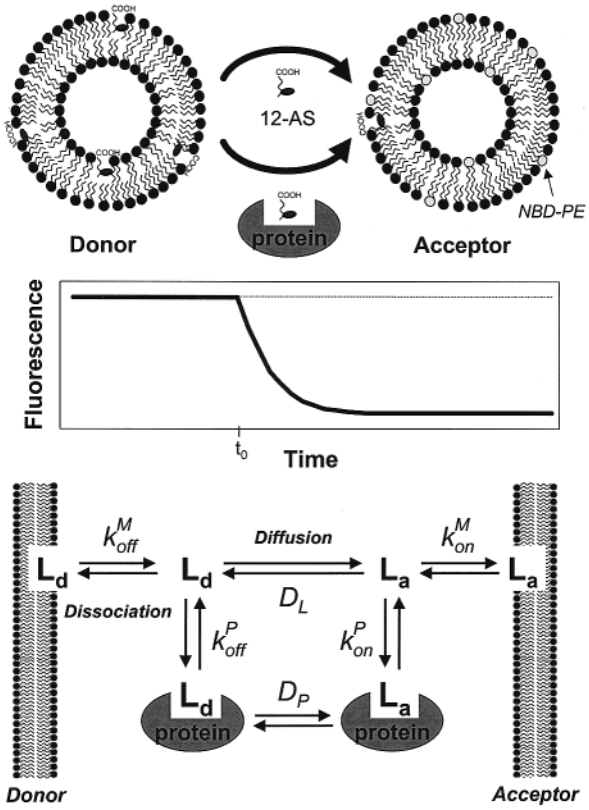

FIGURE 1: Kinetic model of protein-mediated intermembrane ligand diffusion. The upper panel schematically illustrates the experimental system used for monitoring the spontaneous transfer of the fatty acid analogue, 12-anthroyloxy stearate (12-AS), from phosphatidylcholine (●) donor vesicles to acceptor vesicles containing 10 mol % NBD-phosphatidylethanolamine (NBD-PE; ○). At time zero (t_0), 12-AS-containing donor vesicles are rapidly mixed with NBD-labeled acceptor vesicles by stopped-flow techniques. The rate of diffusion of 12-AS from the donor to the acceptor membrane is calculated from the time-dependent quenching of anthroyloxy fluorescence intensity. Experiments are performed in the absence (upper pathway) and presence (lower pathway) of soluble binding proteins. The lower panel depicts the kinetic model developed to describe the diffusion of an amphipathic ligand (L) from a donor membrane (subscript d) to an acceptor membrane (subscript a). The model assumes a diffusional transfer mechanism for the free ligand between the donor and acceptor membranes (upper pathway) and between the membranes and the carrier protein (lower pathway). All molecular species and kinetic parameters are defined in Table 1.

Stopped-Flow Analysis of Intermembrane Fatty Acid Transfer. Anthroyloxy-labeled fatty acids exhibit substantial fluorescence when associated with membrane vesicles composed of phosphatidylcholine (*26*), and it has previously been demonstrated that this fluorescence is efficiently quenched by the incorporation of NBD-PE into the lipid bilayer (*27*). Therefore, by employing an experimental system originally described by Kleinfeld and Storch (*28*), the rate of 12-AS transfer from small unilamellar phosphatidylcholine donor vesicles to acceptor vesicles containing 10 mol % NBD-PE can be accurately measured by monitoring the time-dependent quenching of anthroyloxy fluorescence intensity (Figure 1, upper panel). Since the quantum yield of free 12-AS is trivial as compared with that of membrane-bound probe, and

Table 1: Definition of Terms

term	definition
v	velocity of ligand arrival at the acceptor membrane (mol/s)
$[L_d]$	free ligand concentration near the *donor* membrane (mol/cm^3)
$[L_a]$	free ligand concentration near the *acceptor* membrane (mol/cm^3)
$[M_d]$	concentration of *donor* membrane phospholipid (mol/cm^3)
$[M_a]$	concentration of *acceptor* membrane phospholipid (mol/cm^3)
$[M_d{\cdot}L_d]$	concentration of ligand bound to the *donor* membrane (mol/cm^3)
$[M_a{\cdot}L_a]$	concentration of ligand bound to the *acceptor* membrane (mol/cm^3)
[P]	concentration of free binding protein (mol/cm^3)
$[P{\cdot}L_d]$	concentration of protein-bound ligand near the *donor* membrane (mol/cm^3)
$[P{\cdot}L_a]$	concentration of protein-bound ligand near the *acceptor* membrane (mol/cm^3)
K^{M}_{a}	affinity constant of the membrane for the ligand (cm^3/mol)
K^{P}_{a}	affinity constant of the binding protein for the ligand (cm^3/mol)
k^{M}_{off}	rate constant for the dissociation of ligand from membrane (1/s)
k^{P}_{off}	rate constant for the dissociation of ligand from binding protein (1/s)
k^{M}_{on}	rate constant for the association of ligand with membrane [cm^3/(mol·s)]
k^{P}_{on}	rate constant for the association of ligand with binding protein [cm^3/(mol·s)]
d	diffusion distance (cm)
δ	depth of unstirred water layer (cm) [considered equivalent to d]
V_d	volume within which diffusion occurs (cm^3)
S	membrane surface area (cm^2) [equivalent to V_d/d]
D_L	diffusion coefficient of the ligand (cm^2/s)
D_P	diffusion coefficient of the binding protein (cm^2/s)

since the concentration of free probe is exceedingly low under the conditions utilized (*27*), changes in probe fluorescence directly reflect 12-AS arrival at the acceptor membrane.

An Aminco-Bowman II fluorescence spectrophotometer equipped with an SLM-Aminco MilliFlow reactor (mixing time 20 ms) facilitated the rapid mixing of donor and acceptor vesicles. Excitation and emission wavelengths were 383 and 455 nm, respectively, and a standard sampling interval of 200 ms was employed in all studies. The use of excitation and emission slits of 2 and 8 nm resulted in minimal photobleaching, which had no significant impact on the results. As it previously has been shown that the intermembrane transfer of anthroyloxy fatty acids is best described by two exponentials (*27*, *29*), the time course for changes in 12-AS fluorescence was analyzed by fitting the fluorescence curves to both single- and double-exponential functions, as previously described (*24*, *30*). Quality of fit was assessed by regression analysis, and an *F*-test was applied to determine if the inclusion of an additional term provided a statistically significant improvement in curve fit. To facilitate testing of the experimental model, data also are plotted in terms of the initial velocity of 12-AS arrival, calculated from the slope of the transfer curve at 2 s.

The incorporation of 12-AS into donor vesicles was accomplished by solubilizing the fluorescent probe in ethanol and adding a small aliquot (<0.1 vol %) to the vesicle suspension (*27*, *28*). For studies of protein-mediated fatty acid transport, binding proteins were preequilibrated with a suspension of acceptor vesicles prior to stopped-flow mixing, unless otherwise indicated. In a standard experiment, the final concentration of 12-AS was 1 μM, and donor and acceptor vesicle phospholipid concentrations were 50 and 100 μM, respectively. Minor variations in rate measurements between experiments were experienced as a result of imprecisions in the measured lipid concentration of independently prepared stock solutions. In an effort to reduce this type of variability, a single stock solution of sonicated donor and acceptor vesicles was utilized for each set of experiments.

Kinetic Model of Intermembrane Ligand Transport. The case in which intermembrane ligand transfer occurs in the *absence* of binding proteins is first considered (Figure 1, lower panel). The mathematical derivations are based on the assumption that all ligand is localized to the donor (e.g., plasma) membrane at the start of the experiment and that initial rate conditions prevail, such that the concentration of ligand bound to the acceptor (e.g., endoplasmic reticulum) membrane, $[M_a{\cdot}L_a]$, equals zero. All terms used in this and subsequent derivations are detailed in Table 1. As it previously has been shown that the intermembrane transfer of fatty acids occurs by aqueous diffusion of free fatty acid monomers rather than via collisions between donor and acceptor membranes (*27*), the initial velocity (v) of ligand arrival at the *acceptor* membrane can be expressed as

$$v = \frac{d[M_a{\cdot}L_a]}{dt} = k^{M}_{on} V_d [M_a][L_a] \quad (1)$$

where k^{M}_{on} reflects the on-rate constant for ligand binding to the acceptor (or donor) membrane, V_d is the volume within which diffusion occurs, $[M_a]$ is the acceptor membrane concentration, and $[L_a]$ is the concentration of free ligand in the vicinity of the acceptor membrane. If one further assumes that the concentration of free ligand near the *donor* membrane, $[L_d]$, reaches steady state rapidly and remains constant during the initial transfer rate measurements (i.e., rapid equilibrium) (*31*, *32*), then

$$\frac{d[L_d]}{dt} = k^{M}_{off} V_d [M_d{\cdot}L_d] - k^{M}_{on} V_d [L_d][M_d] - \frac{S}{\delta} D_L [L_d] + \frac{S}{\delta} D_L [L_a] = 0 \quad (2)$$

where $[M_d]$ and $[M_d{\cdot}L_d]$ are the concentrations of donor membrane and the donor membrane−ligand complex, respectively, k^{M}_{off} is the off-rate constant for the ligand from the donor (or acceptor) membrane, S is the external surface area of the vesicles, δ is the depth of the unstirred water layer (*33*), and D_L is the diffusion coefficient for the ligand.

Assuming the affinity of the ligand for the donor membrane is equivalent to that for the acceptor membrane, then the equilibrium affinity constant $K^{M}{}_{a}$ can be written as

$$K^{M}{}_{a} = \frac{[M_d \cdot L_d]}{[M_d][L_d] + [M_a][L_a]} \quad (3)$$

Solving eq 3 for $[L_d]$ and substituting into eq 2 yields

$$[L_a] = \frac{\frac{S}{\delta}D_L[M_d \cdot L_d]}{k^{M}{}_{on}V_d K^{M}{}_{a}[M_d][M_a] + \frac{S}{\delta}D_L K^{M}{}_{a}[M_d] + \frac{S}{\delta}D_L K^{M}{}_{a}[M_a]} \quad (4)$$

Within the cell, the diffusion distance (d), which is equivalent to V_d/S, can reasonably be assumed to be equivalent to δ. Upon substitution for $[L_a]$ in eq 1, the inverse velocity of ligand arrival at the acceptor membrane, in the absence of binding proteins, is given by

$$\frac{1}{v} = \left[\frac{d^2 K^{M}{}_{a}[M_d]}{D_L} + \left(1 + \frac{[M_d]}{[M_a]}\right)\frac{1}{k^{M}{}_{off}}\right]\frac{1}{V_d[M_d \cdot L_d]} \quad (5)$$

If the concentration of donor membranes is maintained constant, the influence of the acceptor membrane concentration on the velocity of intermembrane ligand transfer is described by the following general solution to eq 5:

$$v = \frac{1}{\left(\frac{C_1}{[M_a]} + C_2\right)} \quad (6)$$

where C_1 and C_2 are constant terms. On the basis of this equation, it is anticipated that the ligand transfer rate will increase asymptotically with $[M_a]$.

Kinetics of Protein-Mediated Ligand Transport. The case in which intermembrane ligand transfer occurs in the *presence* of a soluble binding protein is now considered. Bovine serum albumin has been utilized as a model binding protein in several FRAP studies of intracellular diffusion (*9*, *10*). As it previously has been shown that the transfer of fatty acids between membrane vesicles and BSA occurs via aqueous diffusion (*34*), a kinetic model of protein-mediated intermembrane ligand transport was developed in which a diffusional mechanism of ligand−protein interaction is assumed (Figure 1, lower panel). Under these conditions, the time-dependent change in free ligand concentration near the donor membrane can be expressed as

$$\frac{d[L_d]}{dt} = k^{M}{}_{off}V_d[M_d \cdot L_d] - k^{M}{}_{on}V_d[L_d][M_d] - k^{P}{}_{on}V_d[P][L_d] + k^{P}{}_{off}V_d[P \cdot L_d] - \frac{S}{\delta}D_L[L_d] + \frac{S}{\delta}D_L[L_a] \quad (7)$$

where [P] represents the concentration of free protein, $[P \cdot L_d]$ reflects the concentration of ligand-bound protein near the donor membrane, and $k^{P}{}_{on}$ and $k^{P}{}_{off}$ are the on- and off-rate constants for the ligand from the protein. Similarly, the change in concentration of the protein−ligand complex near the donor membrane over time can be written as

$$\frac{d[P \cdot L_d]}{dt} = k^{P}{}_{on}V_d[P][L_d] - k^{P}{}_{off}V_d[P \cdot L_d] - \frac{S}{\delta}D_p[P \cdot L_d] + \frac{S}{\delta}D_p[P \cdot L_a] \quad (8)$$

where $[P \cdot L_a]$ indicates the concentration of ligand-bound protein near the acceptor membrane and D_p represents the diffusion coefficient of the protein. Assuming rapid equilibrium, such that

$$\frac{d[L_d]}{dt} = \frac{d[P \cdot L_d]}{dt} = 0$$

and expressing the equilibrium affinity constant of the protein for the ligand as

$$K^{P}{}_{a} = \frac{[P \cdot L_d] + [P \cdot L_a]}{[P][L_d] + [P][L_a]} \quad (9)$$

we obtain the following velocity equation:

$$\frac{1}{v} = \left[\left(1 + \frac{\mathbf{2}\boldsymbol{D_P}}{\boldsymbol{d^2 k^{P}_{off}}}\right)\frac{d^2 K^{M}{}_{a}[M_d]}{D_L} + \left(1 + \frac{\mathbf{2}\boldsymbol{D_P}}{\boldsymbol{d^2 k^{P}_{off}}} + \frac{\boldsymbol{D_P K^{P}_{a}[P]}}{\boldsymbol{D_L}}\right)\left(1 + \frac{[M_d]}{[M_a]}\right)\frac{1}{k^{M}{}_{off}}\right]\frac{1}{V_d[M_d \cdot L_d]} \quad (10)$$

Examination of eq 10 reveals that, for a diffusional mechanism of ligand−protein interaction, the additional terms generated by the presence of a carrier protein (shown in boldface type) can only result in a *decrease* in the initial velocity of ligand arrival at the acceptor membrane. If donor and acceptor membrane concentrations are maintained constant, eq 10 can be simplified to the following general solution:

$$v = \frac{1}{C_3[P] + C_4} \quad (11)$$

where C_3 and C_4 are constants comprising the following combination of parameters:

$$C_3 = \frac{D_p K^{P}{}_{a}}{D_L}\left(1 + \frac{[M_d]}{[M_a]}\right)\left(\frac{1}{k^{M}{}_{off}}\right)\left(\frac{1}{V_d[M_d \cdot L_d]}\right)$$

$$C_4 = \left[\left(\frac{d^2 K^{M}{}_{a}[M_d]}{D_L}\right) + \left(1 + \frac{[M_d]}{[M_a]}\right)\left(\frac{1}{k^{M}{}_{off}}\right)\right] \times \left(1 + \frac{2D_P}{d^2 k^{P}{}_{off}}\right)\left(\frac{1}{V_d[M_d \cdot L_d]}\right)$$

On the basis of eq 11, an asymptotic decline in the velocity of ligand intermembrane transfer is predicted as the concentration of binding protein is increased.

RESULTS

In an attempt to validate the derived model of intermembrane ligand transfer (eq 5), we utilized the fluorescent fatty

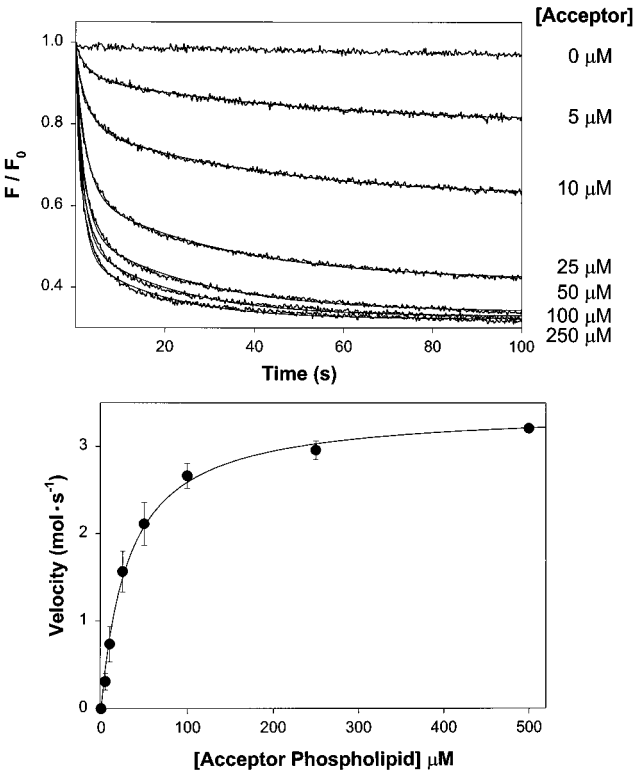

FIGURE 2: Effect of acceptor vesicle phospholipid concentration on the rate of 12-AS intermembrane diffusion. In the upper panel, the spontaneous transfer of 12-AS (1 μM) from phosphatidylcholine donor vesicles (50 μM phospholipid) to 10 mol % NBD-labeled acceptor vesicles is recorded over a range of acceptor concentrations (0−250 μM phospholipid). Each curve reflects the average of four stopped-flow injections performed at 25 °C and is expressed as the ratio of 12-AS fluorescence intensity (F) versus initial fluorescence at time 0 (F_0). As previously reported (*27*), curves are best described ($p < 0.0005$) by a double-exponential function (solid lines). In the lower panel, the 12-AS transfer velocity at 2 s is plotted against the acceptor vesicle phospholipid concentration (0−500 μM). Each point represents the mean ± SD of three separate sets of stopped-flow injections. The data are fit to eq 6 (solid line, $p < 0.0005$), producing values for the constants C_1 and C_2 of 0.094 ± 0.007 s/cm^3 and (2.92 ± 0.07) × 10^6 s/mol (±SE), respectively.

acid probe, 12-anthroyloxy stearate (12-AS), as a representative amphipathic ligand. The upper panel of Figure 2 displays the results of a series of stopped-flow recordings of the spontaneous transfer of 12-AS from small unilamellar phosphatidylcholine vesicles to varying concentrations of 10% NBD-PE-labeled acceptor vesicles, conducted in the absence of binding proteins. The finding that no detectable transfer signal is observed in the absence of acceptor vesicles (Figure 2, upper panel) verifies that the contribution of free 12-AS to the overall signal is negligible and can reasonably be ignored under the conditions employed in these studies. This finding is not surprising in light of the low aqueous solubility and high K_a for 12-AS binding to phospholipid vesicles (*35*). Consistent with previous reports (*27*, *28*), transfer curves are best described by a double-exponential function, with the fast component of transfer reflecting dissociation of the fatty acid probe from the external bilayer leaflet and the slow phase representing transbilayer flip-flop (*27*, *28*). When plotted against the acceptor vesicle concentration, the initial velocity of 12-AS transfer increases asymptotically with the concentration of acceptor vesicle phospholipid (Figure 2, lower panel), consistent with the proposed model.

Mechanism of 12-AS Transfer between Bovine Serum Albumin and Phospholipid Vesicles. Since bovine serum albumin (BSA) has been employed as a model binding protein in studies of fatty acid diffusion (*9*, *10*), we sought to examine the effect of this protein on the kinetics of 12-AS intermembrane transfer. The outlined model of protein-mediated ligand diffusion (eq 10) assumes that ligand transfer between membrane and protein occurs via aqueous diffusion. While it previously has been shown that the transfer of myristate between BSA and membrane vesicles occurs by this mechanism (*34*), we sought to validate these findings for the fluorescent fatty acid analogue (12-AS) used in the present studies. The mechanism of ligand transfer can be deduced by measuring transfer rates in the presence of varying donor and/or acceptor concentrations (*22*, *32*). For a collisional process, the transfer rate increases in a linear fashion in conjunction with either the donor or acceptor concentration. Conversely, the rate of diffusion-mediated transfer asymptotically approaches the dissociation rate from the acceptor as the donor:acceptor ratio rises. Since the quantum yield of 12-AS is markedly enhanced on binding to bovine serum albumin, the transfer of 12-AS from BSA to NBD-labeled acceptor vesicles was analyzed by an approach similar to that employed in the study of 12-AS intermembrane diffusion (Figure 3, upper panel). Transfer curves again were found to be best described by a double-exponential function, with the slow component of transfer likely reflecting flip-flop of the probe at the *acceptor* membrane. An asymptotic decline in the rate of 12-AS transfer is observed as the molar ratio of donor BSA to acceptor phospholipid increases (Figure 3, lower panel), consistent with a diffusional transfer mechanism (*36*).

Effect of Bovine Serum Albumin on the Intermembrane Transfer of 12-AS. To determine the effect of bovine serum albumin on the rate of intermembrane ligand transfer, varying concentrations of BSA were added to a suspension of NBD-labeled acceptor vesicles prior to stopped-flow mixing with donor vesicles containing 12-AS (Figure 4, upper panel). As predicted by eq 11, there is a coincident decline in the rate of 12-AS intermembrane transfer as the concentration of BSA is increased (Figure 4, lower panel). Similar results were obtained when BSA was preequilibrated with the donor, rather than the acceptor, vesicles (Figure 5). To control for confounding effects arising from potential changes in 12-AS fluorescence intensity when bound to BSA, the transfer of 12-AS from phosphatidylcholine donor vesicles to BSA was examined by stopped-flow techniques (Figure 6, upper panel). Under these conditions, a change in the quantum yield of membrane- versus protein-bound 12-AS will be reflected by a time-dependent change in anthroyloxy fluorescence. The observation that the fluorescence intensity of 12-AS bound to donor vesicles is unaffected by the presence or absence of BSA indicates that the quantum yield is similar for membrane- and protein-bound probe. These findings further validate the experimental system, confirming that quenching of 12-AS fluorescence intensity occurs only in the presence of NBD-labeled acceptor vesicles.

Influence of Liver and Intestinal Fatty Acid-Binding Proteins on the Kinetics of 12-AS Diffusion. To assess whether data obtained with bovine serum albumin are

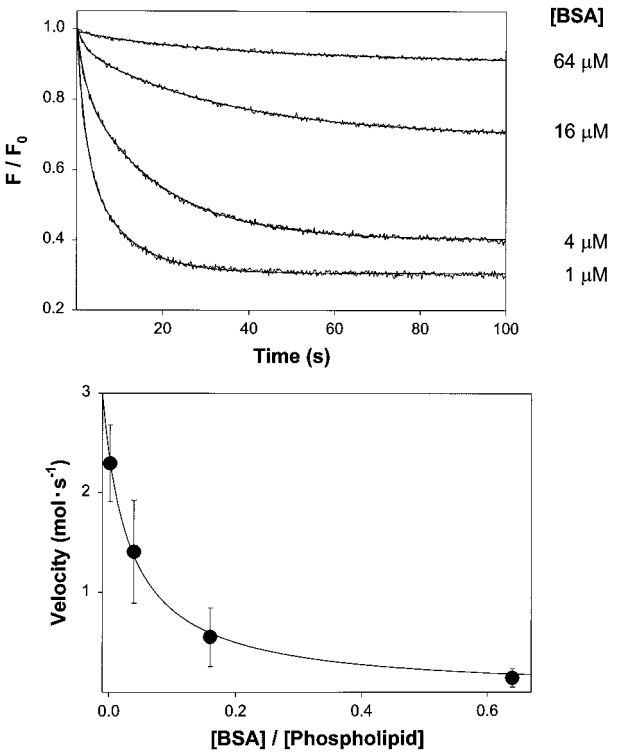

FIGURE 3: Transfer of 12-AS from BSA to membrane vesicles: influence of the albumin concentration. The upper panel displays representative fluorescence recordings of 12-AS (1 μM) transfer from varying concentrations (1−64 μM) of bovine serum albumin (BSA) to small unilamellar phosphatidylcholine acceptor vesicles containing 10% NBD-PE (100 μM phospholipid). Tracings represent the average of four stopped-flow injections performed at 25 °C and are best described by a double-exponential function (solid lines). In the lower panel, a plot of the 12-AS transfer velocity at 2 s versus the molar ratio of BSA to acceptor vesicle phospholipid exhibits an asymptotic decline, consistent with a diffusional transfer mechanism. Data points reflect the mean ± SD of three sets of experiments and are fit to a previously described model of diffusional transfer (*36*).

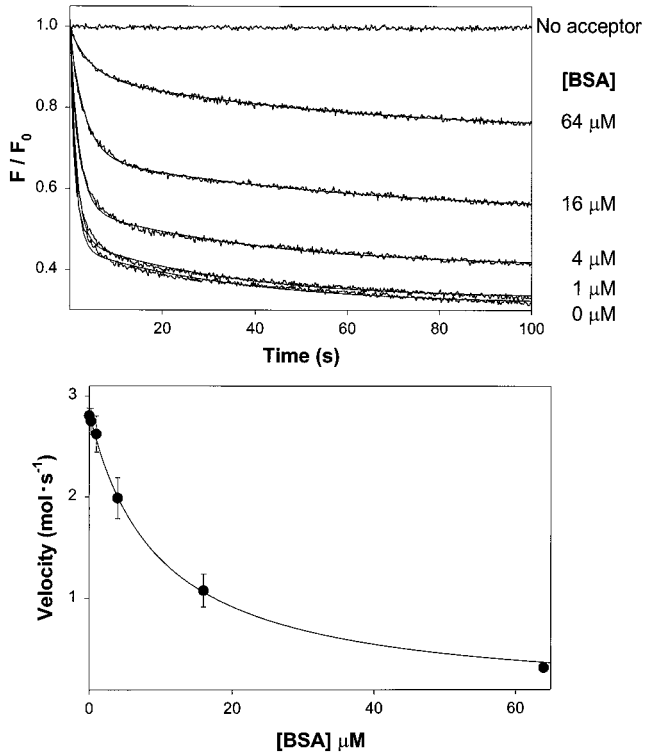

FIGURE 4: Effect of BSA on the rate of 12-AS diffusion between membrane vesicles. The upper panel displays a series of fluorescence recordings of 12-AS (1 μM) transfer from phosphatidylcholine donor vesicles (50 μM phospholipid) to a suspension of NBD-labeled acceptor vesicles (100 μM phospholipid) preincubated with varying concentrations (0−64 μM) of bovine serum albumin (BSA). Each curve represents the average of four stopped-flow injections performed at 25 °C and is fit to a double-exponential equation (solid lines). No time-dependent changes in fluorescence intensity are observed in the absence of acceptor membranes. In the lower panel a plot of the transfer velocity (±SD) versus the BSA concentration is shown. The solid line reflects the fit to eq 11 ($p < 0.0005$), which produces values for C_3 and C_4 of $(3.7 \pm 0.2) \times 10^{14}$ cm^3·s/mol^2 and $(3.53 \pm 0.03) \times 10^6$ s/mol (±SE), respectively.

generalizable to other soluble binding proteins, additional experiments examining the influence of fatty acid-binding proteins on 12-AS intermembrane diffusion were performed. Liver and intestinal FABP were selected for analysis because these two proteins previously have been shown to bind and transport 12-AS via different mechanisms (*37*). Control studies again demonstrate that binding to liver (Figure 6, lower panel) or intestinal (data not shown) FABP does not appreciably alter 12-AS fluorescence intensity as compared with membrane-bound probe. Preincubation of acceptor vesicles with L-FABP, which transports fatty acids via a diffusional mechanism (*38*, *39*), causes a modest, concentration-dependent decrease in the rate of 12-AS intermembrane transfer (Figure 7), analogous to results obtained with BSA. In contrast, when I-FABP, which previously has been shown to exhibit a collisional transport mechanism (*37*), is preincubated with acceptor vesicles, the rate of 12-AS transfer from donor to acceptor membranes increases in a linear fashion with the protein concentration (Figure 8).

DISCUSSION

The outlined model of intermembrane ligand transport (eq 9) predicts that soluble proteins that exhibit diffusional binding kinetics (e.g., BSA, L-FABP) will slow the rate of intermembrane ligand transport. The results of experiments examining the intermembrane transfer of the fluorescent fatty acid analogue 12-AS in the presence of BSA and L-FABP are entirely consistent with the proposed model. Indeed, these findings intuitively make sense in light of the fact that, for most amphipathic ligands (e.g., fatty acids, phospholipids), solvation from the donor particle represents the rate-limiting step in the transfer process (*40*−*43*). A collisional transfer mechanism involves direct contact between the protein and the donor membrane. If the interaction of the protein at the membrane surface causes a reduction in the energetic barrier to ligand dissociation, an enhanced rate of transfer should result (*43*−*45*). Therefore, proteins that exhibit a collisional mechanism (e.g., adipocyte FABP, phosphatidylcholine transfer protein) would be expected to *increase* the rate of arrival at the acceptor membrane, as was observed with I-FABP. In the case of diffusional transport, there is no direct interaction between membrane and protein; hence, dissociation of ligand from the donor membrane (or arrival at the acceptor membrane) cannot be facilitated.

Vork et al. (*45*) developed a computer model of intracellular flux in which the effect of a soluble binding protein on ligand translocation from one membrane to another is considered. On the basis of results of computer simulations, these authors proposed that the rate of ligand transfer from

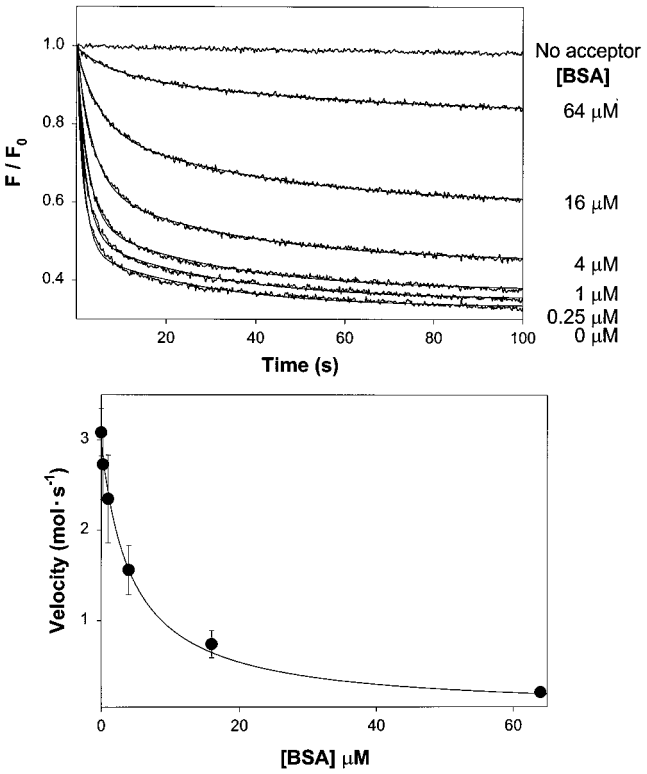

FIGURE 5: Effect of preincubating donor vesicles with BSA on the rate of 12-AS intermembrane transfer. In the upper panel, data from a series of experiments examining the effect of bovine serum albumin (BSA) on the rate of transfer of 12-AS between small unilamellar phosphatidylcholine donor vesicles and 10 mol % NBD-labeled acceptor vesicles are displayed. The experimental conditions are identical to those described in Figure 4, with the exception that the BSA (0−64 μM) was preequilibrated with the 12-AS-containing *donor* vesicles prior to stopped-flow mixing. In the lower panel, the rate of 12-AS transfer (±SD) is plotted against the BSA concentration ($n = 3$). The data are fit to eq 11 (solid line, $p < 0.0005$), with $C_3 = (7.5 \pm 0.8) \times 10^{14}$ cm^3·s/mol^2 and $C_4 = (3.37 \pm 0.08) \times 10^6$ s/mol (±SE).

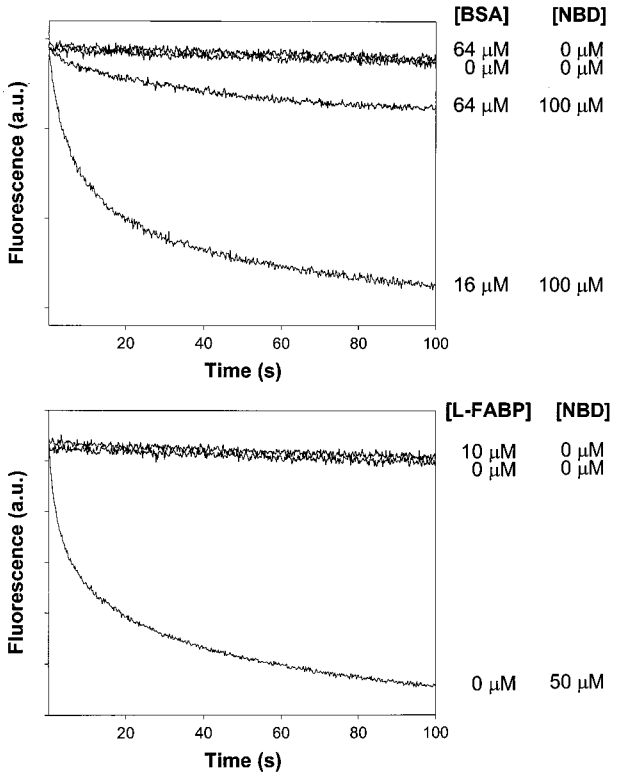

FIGURE 6: Influence of protein binding on 12-AS fluorescence intensity. In the upper panel, recordings of 12-AS (1 μM) fluorescence when bound to small unilamellar phosphatidylcholine donor vesicles (50 μM phospholipid) were obtained following stopped-flow mixing with varying concentrations of NBD-labeled acceptor vesicles (NBD) and/or bovine serum albumin (BSA). Fluorescence intensity is expressed in arbitrary units (au). The upper two tracings were obtained in the absence of acceptor vesicles and demonstrate that the signal intensity for BSA-bound 12-AS is similar to that for membrane-bound probe. The addition of NBD-labeled acceptor vesicles (lower curves) results in a time-dependent decrease in fluorescence signal, due to quenching of 12-AS fluorescence intensity following the spontaneous transfer of the probe to the acceptor membranes. Fluorescence intensities are corrected for inner filter and light-scattering effects of the NBD-labeled vesicles. The lower panel displays the results of similar studies in which BSA is replaced by liver fatty acid-binding protein (L-FABP).

donor to acceptor membrane is linearly related to the protein concentration under the condition where collisional interactions occur at both membranes. Furthermore, in the situation where no collisional interactions were allowed (i.e., diffusional transport), ligand translocation was found to be solely determined by the rate of spontaneous dissociation of the ligand from the donor membrane. While their model does not account for a concentration-dependent *decrease* in the rate of intermembrane ligand transfer when a diffusional transport mechanism is operational, the general conclusions reached by these investigators are largely consistent with our findings.

Previous studies of myristate transfer between unilamellar vesicles composed of dimyristoylphosphatidylcholine and bovine serum albumin indicate a diffusional mechanism of fatty acid exchange (*34*). Our findings with respect to the kinetics of 12-AS transfer from BSA to NBD-labeled phosphatidylcholine vesicles provide further confirmation of these results. Data regarding the mechanism of liver FABP-mediated fatty acid transport are more controversial. While a majority of studies support a diffusional mechanism of fatty acid transfer (*37*−*39*), other investigators have shown that the binding of L-FABP to anionic lipid vesicles results in ligand release (*46*), consistent with a collisional transport mechanism. Although our analyses cannot exclude the possibility that two transport mechanisms are simultaneously operational, the observed decrease in the rate of intermembrane 12-AS transfer with increasing protein concentration (Figure 7) supports a predominantly diffusional mechanism of L-FABP-mediated transport of neutral membrane lipids. Our data further indicate that I-FABP transports fatty acids via a mechanism distinct from that for L-FABP and are consistent with prevailing evidence that this process involves protein−membrane collisions (*37*, *47*). It is notable that enterocytes express both intestinal and liver isoforms of FABP. The fact that the expression of L- and I-FABP is differentially regulated (*48*) and that the proteins exhibit distinct transport mechanisms suggests a unique cellular function for these two FABP isoforms (*37*).

Our findings contradict the results of FRAP studies, which have consistently demonstrated that both BSA and L-FABP enhance the rate of fatty acid diffusion in model cytoplasm (*9*, *10*), as well as in permeabilized (*9*) and intact (*11*−*13*, *15*) cells. In an attempt to explain these discrepant observations, Weisiger (*10*) has suggested that binding proteins are not required for the "short" intermembrane transfer distances

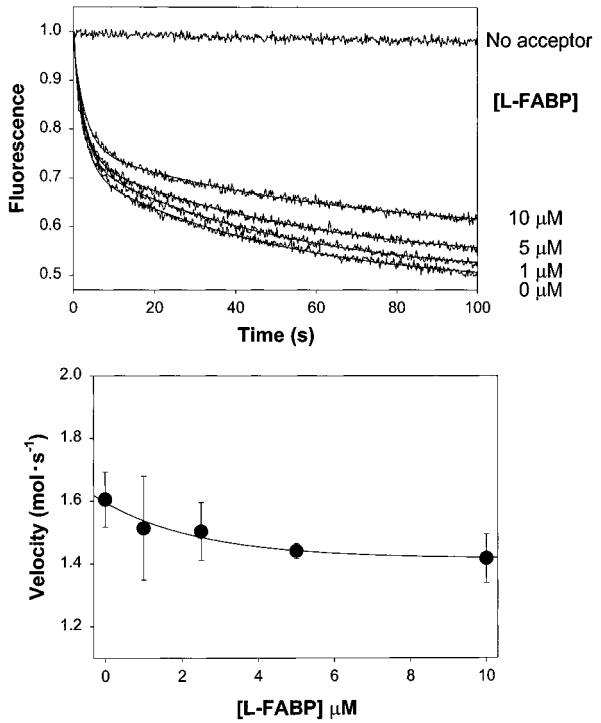

FIGURE 7: Effect of liver FABP on the diffusion of 12-AS between membrane vesicles. The upper panel displays representative fluorescence recordings of the transfer of 12-AS (1 μM) from phosphatidylcholine donor vesicles (50 μM phospholipid) to NBD-labeled acceptor vesicles (50 μM phospholipid) in the presence of varying concentrations (0−10 μM) of liver fatty acid-binding protein (L-FABP). Each curve represents the average of four stopped-flow injections performed at 25 °C and is fit to a double-exponential equation (solid line). Again, there is no change in fluorescence in the absence of acceptor vesicles. In the lower panel, the 12-AS transfer velocity (±SD) is plotted versus the concentration of L-FABP ($n = 3$), with the data fit to eq 11 (solid line, $p < 0.05$). Values obtained for the constants C_3 and C_4 are $(8 \pm 2) \times 10^{13}$ cm^3·s/mol^2 and $(6.4 \pm 0.1) \times 10^6$ s/mol (±SE), respectively.

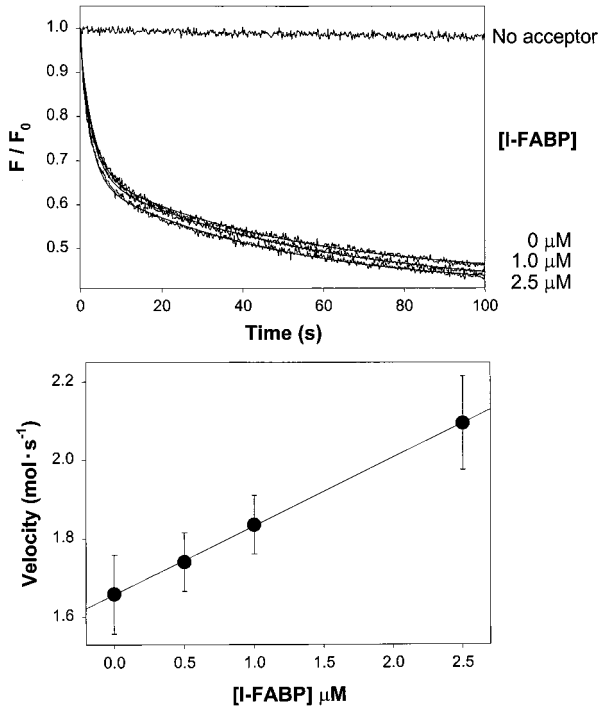

FIGURE 8: Influence of intestinal FABP on the kinetics of 12-AS intermembrane diffusion. The upper panel displays tracings of 12-AS intermembrane transfer in the presence of varying concentrations (0−2.5 μM) of intestinal fatty acid-binding protein (I-FABP), along with double-exponential fits (solid lines). Conditions are identical to those described in Figure 7. In the lower panel, it is observed that the 12-AS transfer velocity (±SD) increases linearly with the concentration of I-FABP ($n = 4$). Since eq 11 is unable to account for a rise in the transfer rate, the solid line reflects a linear fit of the data ($p < 0.0005$).

present in experimental systems in which ligand transfer between model or isolated native membrane vesicles is examined. He has further postulated that, for the sufficiently large distances present within the cell (i.e., greater than $\sqrt{D_L/k^M_{on}}$), the diffusion of amphipathic compounds is greatly enhanced by binding proteins (*10*). In support of this hypothesis, liver FABP has been shown to increase the rate of fatty acid transport when donor and acceptor membrane compartments are separated by a filter (*49*, *50*). However, the proposed mathematical model is unable to account for the concentration-dependent *decline* in the rate of intermembrane ligand transfer observed in the present experiments.

While the diffusion distances present in our vesicle transfer studies (~0.9 μm for 100 μM phospholipid) are small relative to the average diameter (~20 μm) of a hepatocyte (*10*), one must take into account the fact that cells contain a myriad of internal membranes. Hence, it is likely that the movement of an amphipathic ligand inside the cell consists of a series of "hops" from one intracellular membrane to another, each event involving distances that are well within the range examined in our stopped-flow system. Moreover, the kinetic model of intermembrane ligand transport outlined in Figure 1 was specifically designed to take into consideration diffusion distance, as well as ligand and protein diffusion coefficients. According to this model, if all other variables are maintained constant, an increase in the distance between donor and acceptor membranes will decrease the velocity of ligand arrival at the acceptor membrane (eq 5). Furthermore, at any given diffusion distance, the addition of a binding protein with a diffusional transfer mechanism is predicted to impede ligand translocation, an effect that is independent of protein concentration (eq 9). On the other hand, at a specified protein concentration, differences in ligand transfer velocity in the presence or absence of a binding protein diminish as the diffusion distance increases toward infinity. Unfortunately, it is difficult to test these predictions because the only way to modulate the distance between membrane vesicles is by modifying the vesicle concentration, which independently affects the ligand transfer rate.

Thus, we are left with a situation in which robust experimental data lead to paradoxical conclusions. FRAP analyses unequivocally support that BSA enhances intracellular fatty acid diffusion, while vesicle transfer studies indicate that this protein inhibits intermembrane fatty acid translocation. A possible explanation for these seemingly incongruous observations may reside in the ligand utilized for study. Both NBD-stearate (employed in FRAP studies) and anthroyloxy stearate (used in the present investigations) are fatty acid analogues, and the attached fluorescent group potentially may alter the physical properties of the molecule as compared with the corresponding native fatty acid. 12-(9-Anthroyloxy)stearic acid was selected for use in the present experiments because this probe has previously been

employed in a number of binding and transfer studies (*37*−*39*, *51*, *52*), and a substantial body of information regarding the physical and kinetic properties of this molecule is available (*26*, *35*, *53*, *54*). Moreover, the partition behavior, transfer properties, and intracellular metabolic fate of anthroyloxy fatty acid analogues are similar to those of native fatty acids (*55*, *56*). While much less is known about the physical properties of NBD-labeled fatty acids, there is evidence to suggest that the presence of the NBD group causes a marked deviation in the orientation of the molecule in membrane bilayers in comparison with native fatty acids (*53*, *57*). On the other hand, although alterations in the physical properties of a ligand conceivably may cause quantitative changes in binding affinity and dissociation rate, it seems less likely to affect the kinetic *mechanism* underlying the ligand−protein interaction.

It must be emphasized that our kinetic model is based on the fundamental assumptions that (1) all ligand initially is bound to the donor membrane (i.e., initial rate), (2) the ligand destination is a membrane, and (3) a rapid equilibrium is reached near the surface of the donor membrane before the concentration of ligand in the donor membrane is significantly depleted. It can be argued that each of these assumptions is generally applicable to conditions inside of the cell. Ligand first appears at the "donor" membrane as a result of diffusion through or transport across the plasma membrane, and rapid metabolism by membrane-based enzymes can reasonably be assumed to instantaneously deplete any ligand arriving at the "acceptor" membrane. Finally, the development of rapid equilibrium near the donor membrane has previously been validated for molecules such as phospholipids (*31*, *32*), which dissociate significantly more slowly than fatty acids. It is notable that the outlined conditions are unquestionably fulfilled in our stopped-flow studies of intervesicle ligand transfer.

While the assumption of rapid equilibrium also is applicable to FRAP analyses, the other stated conditions do not hold. For instance, at the initiation of photobleaching, ligand already is in equilibrium between membranes and binding proteins, with the proportion of protein-bound ligand determined by the concentration of protein introduced into the system. However, this fact alone cannot explain the increased rate of ligand diffusion observed in FRAP studies, as we have shown that preincubation of donor vesicles with BSA still results in a *decreased* rate of intermembrane 12-AS transfer (Figure 6). More importantly, in contrast with intermembrane transfer studies, which monitor ligand arrival at the acceptor vesicle, most FRAP analyses do not distinguish between membrane- and protein-bound ligand. Hence, a substantial proportion of ligand appearing within the photobleached region remains associated with the binding protein, and the velocity of ligand "arrival" is actually described by the more complex expression (as compared with eq 1):

$$v_{\mathrm{FRAP}} = \frac{\mathrm{d}[\mathrm{M_a{\cdot}L_a}]}{\mathrm{d}t} + \frac{\mathrm{d}[\mathrm{P{\cdot}L_a}]}{\mathrm{d}t}$$

It can be argued that protein-bound ligand cannot truly be considered "delivered" since, in the case of diffusional transfer, the protein−ligand complex is unavailable for biotransformation, and dissociation of the ligand from the protein is rate-limiting in many circumstances. Indeed, this is the likely explanation for the surprising finding that, by use of FRAP, an extracellular protein (BSA) appears to be more effective than a cytoplasmic protein (L-FABP) in promoting NBD-stearate diffusion both in model cytoplasm and in permeabilized cells (*9*).

From the above discussion, it is apparent that FRAP studies examine a different end point than vesicle transfer experiments, and this fact may account, at least in part, for the divergent findings obtained by these two methodologies. Furthermore, FRAP analyses assume steady-state conditions (i.e., $[L_d] = [L_a]$), which is not the case for the model outlined in Figure 1. If one puts this information in the context of a cell, stopped-flow experiments are most reflective of an initial ligand bolus, while FRAP studies more closely mimic equilibrium conditions. These important differences probably account for the divergent results obtained by these two methodologies. While it ultimately remains to be determined how these data pertain to normal cellular physiology, our findings validate the derived kinetic model of protein-mediated ligand transport and provide support for the hypothesis that the mechanism of ligand−protein interaction is an important determinant of the effect of soluble proteins on intracellular ligand diffusion.

ACKNOWLEDGMENT

I gratefully acknowledge Dr. Judith Storch for her helpful comments and criticisms and for kindly providing samples of liver and intestinal fatty acid-binding protein. I also thank Dr. Wolfram Goessling and Dr. Richard Weisiger for insightful discussions and Dr. Xiaofa Qin for his technical assistance. Preliminary reports of this work have been published in abstract form (*58*, *59*).

REFERENCES

1. Oude Elferink, R. P. J., Meijer, D. K. F., Kuipers, F., Jansen, P. L. M., Groen, A. K., and Groothuis, G. M. M. (1995) *Biochim. Biophys. Acta 1241*, 215−268.
2. Schroeder, F., Jolly, C. A., Cho, T. H., and Frolov, A. (1998) *Chem. Phys. Lipid. 92*, 1−25.
3. Cerra, F. B., McPherson, J. P., Konstantinides, F. N., Konstantinides, N. N., and Teasley, K. M. (1988) *Surgery 104*, 727−733.
4. Scallen, T. J., Pastuszyn, A., Noland, B. J., Chanderbhan, R., Kharroubi, A., and Vahouny, G. V. (1985) *Chem. Phys. Lipid. 38*, 239−261.
5. Wirtz, K. W. A. (1991) *Annu. Rev. Biochem. 60*, 73−99.
6. Vander Jagt, D. L., Wilson, S. P., Dean, V. L., and Simons, P. C. (1982) *J. Biol. Chem. 257*, 1997−2001.
7. Tipping, E., and Ketterer, B. (1981) *Biochem. J. 195*, 441−452.
8. Weisiger, R. A. (1996) *Hepatology 24*, 1288−1295.
9. Luxon, B. A., and Milliano, M. T. (1997) *Am. J. Physiol. 273*, C859−C867.
10. Weisiger, R. A. (1999) *Am. J. Physiol. 277*, G109−G119.
11. Luxon, B. A., and Milliano, M. T. (1999) *Am. J. Physiol. 277*, G361−G366.
12. Atshaves, B. P., Foxworth, W. B., Frolov, A., Roths, J. B., Kier, A. B., Oetama, B. K., Piedrahita, J. A., and Schroeder, F. (1998) *Am. J. Physiol. 274*, C633−C644.
13. Luxon, B. A. (1996) *Am. J. Physiol. 271*, G113−G120.
14. Murphy, E. J. (1998) *Am. J. Physiol. 275*, G237−G243.
15. Murphy, E. J. (1998) *Am. J. Physiol. 275*, G244−G249.
16. Darimont, C., Gradoux, N., Perohn, E., Cumin, F., and De Pover, A. (2000) *J. Lipid. Res. 41*, 84−92.

17. Runquist, E. A., and Helmkamp, G. M. (1988) *Biochim. Biophys. Acta 940*, 21−32.
18. Cohen, D. E., Leonard, M. R., and Carey, M. C. (1994) *Biochemistry 33*, 9975−9980.
19. Frolov, A., Woodford, J. K., Murphy, E. J., Billheimer, J. T., and Schroeder, F. (1996) *J. Biol. Chem. 271*, 16075−16083.
20. Schroeder, F., Butko, P., Hapala, I., and Scallen, T. J. (1990) *Lipids 25*, 669−674.
21. Gugger, E. T., and Erdman, J. W. (1996) *J. Nutr. 126*, 1470−1474.
22. Zucker, S. D., Goessling, W., Ransil, B. J., and Gollan, J. L. (1995) *J. Clin. Invest. 96*, 1927−1935.
23. DiCorleto, P. E., and Zilversmit, D. B. (1977) *Biochemistry 16*, 2145−2150.
24. Zucker, S. D., Goessling, W., Zeidel, M. L., and Gollan, J. L. (1994) *J. Biol. Chem. 269*, 19262−19270.
25. Bartlett, G. R. (1959) *J. Biol. Chem. 234*, 466−468.
26. Kleinfeld, A. M., and Lukacovic, M. F. (1985) *Biochemistry 24*, 1883−1890.
27. Storch, J., and Kleinfeld, A. M. (1986) *Biochemistry 25*, 1717−1726.
28. Kleinfeld, A. M., and Storch, J. (1993) *Biochemistry 32*, 2053−2061.
29. Kleinfeld, A. M., Chu, P., and Storch, J. (1997) *Biochemistry 36*, 5702−5711.
30. Zucker, S. D., Storch, J., Zeidel, M. L., and Gollan, J. L. (1992) *Biochemistry 31*, 3184−3192.
31. Nichols, J. W., and Pagano, R. E. (1982) *Biochemistry 21*, 1720−1726.
32. Nichols, J. W. (1988) *Biochemistry 27*, 1889−1896.
33. Weisiger, R. A., Pond, S. M., and Bass, L. (1989) *Am. J. Physiol. 257*, G904−G916.
34. Daniels, C., Noy, N., and Zakim, D. (1985) *Biochemistry 24*, 3286−3292.
35. Thulborn, K. R. (1981) in *Fluorescent Probes* (Beddard, G. S., and West, M. A., Eds.) pp 113−141, Academic Press, London.
36. Zucker, S. D., Goessling, W., and Gollan, J. L. (1995) *J. Biol. Chem. 270*, 1074−1081.
37. Hsu, K. T., and Storch, J. (1996) *J. Biol. Chem. 271*, 13317−13323.
38. Kim, H. K., and Storch, J. (1992) *J. Biol. Chem. 267*, 77−82.
39. Storch, J., and Bass, N. M. (1990) *J. Biol. Chem. 265*, 7827−7831.
40. Roseman, M. A., and Thompson, T. E. (1980) *Biochemistry 19*, 439−444.
41. Massey, J. B., Gotto, A. M., and Pownall, H. J. (1982) *Biochemistry 21*, 3630−3636.
42. Nichols, J. W., and Pagano, R. E. (1981) *Biochemistry 20*, 2783−2798.
43. Nichols, J. W. (1985) *Biochemistry 24*, 6390−6398.
44. Nichols, J. W., and Pagano, R. E. (1983) *J. Biol. Chem. 258*, 5368−5371.
45. Vork, M. M., Glatz, J. F. C., and Van der Vusse, G. J. (1997) *Prostaglandins, Leukotrienes Essential Fatty Acids 57*, 11−16.
46. Davies, J. K., Thumser, A. E. A., and Wilton, D. C. (1999) *Biochemistry 38*, 16932−16940.
47. Corsico, B., Cistola, D. P., Frieden, C., and Storch, J. (1998) *Proc. Natl. Acad. Sci. U.S.A. 95*, 12174−12178.
48. Darimont, C., Gradoux, N., Cumin, F., Baum, H. P., and De Pover, A. (1998) *Exp. Cell. Res. 244*, 441−447.
49. Peeters, R. A., Veerkamp, J. H., and Demel, R. A. (1989) *Biochim. Biophys. Acta 1002*, 8−13.
50. McCormack, M., and Brecher, P. (1987) *Biochem. J. 244*, 717−723.
51. Doody, M. C., Pownall, H. J., Kao, Y. J., and Smith, L. C. (1980) *Biochemistry 19*, 108−116.
52. Wootan, M. G., Bernlohr, D. A., and Storch, J. (1993) *Biochemistry 32*, 8622−8627.
53. Abrams, F. S., and London, E. (1993) *Biochemistry 32*, 10826−10831.
54. Abrams, F. S., Chattopadhyay, A., and London, E. (1992) *Biochemistry 31*, 5322−5327.
55. Storch, J., Bass, N. M., and Kleinfeld, A. M. (1989) *J. Biol. Chem. 264*, 8708−8713.
56. Morand, O., Fibach, E., Dagan, A., and Gatt, S. (1982) *Biochim. Biophys. Acta 711*, 539−550.
57. Wolf, D. E., Winiski, A. P., Ting, A. E., Bocian, K. M., and Pagano, R. E. (1992) *Biochemistry 31*, 2865−2873.
58. Zucker, S. D., and Qin, X. (1999) Effect of bovine serum albumin on the intermembrane diffusion of 12-anthroyloxy stearate: implications for the role of soluble proteins in the intracellular transport of hydrophobic ligands, *Hepatology 30*, 464A.
59. Zucker, S. D. (2000) The effect of fatty acid-binding proteins on the intermembrane diffusion of 12-anthroyloxy stearate is determined by the mechanism of ligand−protein interaction, *Hepatology 32*, 441A.

BI001277E